J Musculoskelet Neuronal Interact 2025; 25(3):316-327

Journal of Musculoskeletal and Neuronal Interactions JMNI

Original Article

Construction of a lncRNA–miRNA–mRNA Network for Biomarker Identification in Intervertebral Disc Degeneration

Kai Huang[#1], Lingling Shen[#2], Huiqin Guan[#3], Lei Dai[4], Xiaogang Huang[5], Xinjun Zhang[6], Xiaojun Xu[7], Chao Liu[1]

[1]Department of Orthopedics, Songjiang Hospital Affiliated to Shanghai Jiao Tong University School of Medicine, Shanghai, P.R. China;
[2]Department of Nursing, Shanghai Jiao Tong University School of Medicine Affiliated Shanghai General Hospital, Shanghai, P.R. China;
[3]Shanghai Songjiang District Health Commission, Shanghai, P.R. China;
[4]Department of General Surgery, Songjiang Hospital Affiliated to Shanghai Jiao Tong University School of Medicine, Shanghai, P.R. China;
[5]Department of Gastroenterology, Shanghai Songjiang Sijing hospital, Shanghai, P.R. China;
[6]Department of Orthopedics, Shanghai Songjiang Sijing hospital, Shanghai, P.R. China;
[7]Department of Emergency and Critical Care, Songjiang Hospital Affiliated to Shanghai Jiao Tong University School of Medicine, Shanghai, China
[#]Equal Contribution

Abstract

Objective: To identify pivotal gene markers and pathways involved in intervertebral disc degeneration (IDD) through the construction of a competing endogenous RNA (ceRNA) network. **Methods**: A ceRNA network was constructed using mRNAs associated with clinical IDD phenotypes (age, MRI grade), identified through Weighted Gene Co-expression Network Analysis (WGCNA). From the core mRNAs within the ceRNA network, potential marker genes were identified using LASSO regression, Support Vector Machine (SVM), and Random Forest algorithms. A sub-network was then constructed, and the candidate marker genes were further validated using the mouse IDD dataset GSE134955. **Results**: A total of 119 differentially expressed long non-coding RNAs (DELs), 1,267 differentially expressed mRNAs (DEMs), and 37 differentially expressed microRNAs (DEMis) were identified in IDD samples compared to controls. WGCNA identified 1,190 DEMs significantly associated with MRI grade. Based on these MRI grade-associated DEMs, a hub ceRNA network comprising 4 DEMis, 90 DELs, and 18 DEMs was established. Among these, three DEMs—BTG2, MDM4, and ACOX1—were consistently identified as marker genes by LASSO, SVM, and Random Forest. These three genes also demonstrated high accuracy in distinguishing IDD from control samples in the independent mouse dataset. **Conclusion**: This study identified key mRNAs implicated in IDD progression and provides new insights into the regulatory roles of ceRNA networks in the disease. These findings may contribute to the development of novel diagnostic biomarkers and therapeutic targets for IDD.

Keywords: ceRNA Network, Differential Expressed Genes, Intervertebral Disc Degeneration, mRNAs

The authors have no conflict of interest.

Corresponding authors:
Chao Liu, Department of Orthopedics, Songjiang Hospital Affiliated to Shanghai Jiao Tong University School of Medicine, No.746 Middle Zhongshan Road, Songjiang District, Shanghai, 201600, P.R. China, P.R. China.
E-mail: ortholiuchao2@163.com
Xiaojun Xu, Department of Emergency and Critical Care, Songjiang Hospital Affiliated to Shanghai Jiao Tong University School of Medicine, Shanghai 201600, China
E-mail: Xxj891010@163.com

Edited by: G. Lyritis
Accepted 21 March 2025

Introduction

Intervertebral disc degeneration (IDD) is a leading cause of chronic low back pain (LBP) and disability, particularly in the aging population. Degenerative spine disease and its secondary complications affect an estimated 266 million individuals worldwide, with the highest incidence rates reported in Europe (5.7%) and North America (4.5%)[1]. The pathological basis of IDD includes degradation of the extracellular matrix (ECM) in healthy discs, fibrosis and dehydration of the nucleus pulposus (NP), structural alterations to the cartilaginous endplate, and disrupted

Table 1. The information of dataset.

Sample	Gender	Age	MRI grade	Source data	Group
Control1	Female	35	2	GSE167199	Control
Control2	Male	31	1	GSE167199	Control
Control3	Female	29	1	GSE167199	Control
Case1	Male	57	4	GSE167199	Case
Case2	Male	65	5	GSE167199	Case
Case3	Female	62	5	GSE167199	Case
GSM1354764	Female	33	1	GSE56081/GSE63492	Control
GSM1354765	Female	35	1	GSE56081/GSE63492	Control
GSM1354766	Female	41	1	GSE56081/GSE63492	Control
GSM1354767	Male	43	1	GSE56081/GSE63492	Control
GSM1354768	Female	52	1	GSE56081/GSE63492	Control
GSM1354769	Male	32	4	GSE56081/GSE63492	Case
GSM1354770	Female	38	4	GSE56081/GSE63492	Case
GSM1354771	Female	42	5	GSE56081/GSE63492	Case
GSM1354772	Female	45	4	GSE56081/GSE63492	Case
GSM1354773	Male	27	5	GSE56081/GSE63492	Case

crosstalk with the adjacent subchondral bone[2]. Current treatments for IDD-related LBP primarily involve anti-inflammatory medications, analgesics, and surgical interventions. However, these therapies mainly alleviate symptoms rather than delay disease progression or restore spinal function[3]. Therefore, novel therapeutic strategies and further investigation into the underlying mechanisms of IDD are needed.

Non-coding RNAs, such as long non-coding RNAs (lncRNAs) and microRNAs (miRNAs), are recognized as pivotal regulators of gene expression in various disease processes[4]. miRNAs are short, single-stranded molecules that typically suppress gene expression by binding to target mRNAs, leading to translational repression or degradation[5]. In contrast, lncRNAs are significantly longer and often regulate gene transcription, including the modulation of mRNA production[6]. Both lncRNAs and miRNAs have been identified as important markers in degenerative nucleus pulposus (NP) cells and have been implicated in the progression of intervertebral disc degeneration. For example, lncRNA *HOTAIR* is downregulated in degenerative NP tissues and has been shown to inhibit TNF-α–induced apoptosis in NP cells by modulating miR-34a and *Bcl-2* expression[7]. Similarly, lncRNA *HCG18* has been reported to promote IDD progression by sponging miR-146a-5p and regulating the expression of its target gene *TRAF6*[8]. These findings highlight the importance of interactions among mRNAs, lncRNAs, and miRNAs within competing endogenous RNA (ceRNA) networks, which offer new perspectives for exploring regulatory mechanisms in IDD[9]. Since the construction of ceRNA networks typically relies on selecting genes involved in both lncRNA–mRNA and miRNA–mRNA interactions from sets of differentially expressed lncRNAs (DELs), mRNAs (DEMs), and miRNAs (DEMis), this approach holds promise for identifying novel diagnostic and therapeutic biomarkers in IDD[10].

In this study, we utilized public datasets GSE56081, GSE63492, GSE167199, and GSE134955 to identify candidate marker genes associated with IDD. Candidate genes were initially explored through the construction of a ceRNA network, based on IDD-associated genes identified via Weighted Gene Co-expression Network Analysis (WGCNA). Final key genes were then selected using Least Absolute Shrinkage and Selection Operator (LASSO), Support Vector Machine (SVM), and Random Forest algorithms, and subsequently validated in an independent IDD dataset. The objective of this research is to identify regulatory ceRNA interactions and to infer potential therapeutic targets and underlying mechanisms involved in IDD. These findings may offer valuable insights and contribute to the development of novel strategies for IDD treatment.

Materials and Methods

Data Resource

Transcriptomic and genomic profiles of degenerative nucleus pulposus (NP) tissues were obtained from the Gene Expression Omnibus (GEO) database using the keywords “nucleus pulposus” and “intervertebral disc degeneration.” Four datasets were retrieved, and associated clinical information—including age, gender, and MRI grade—

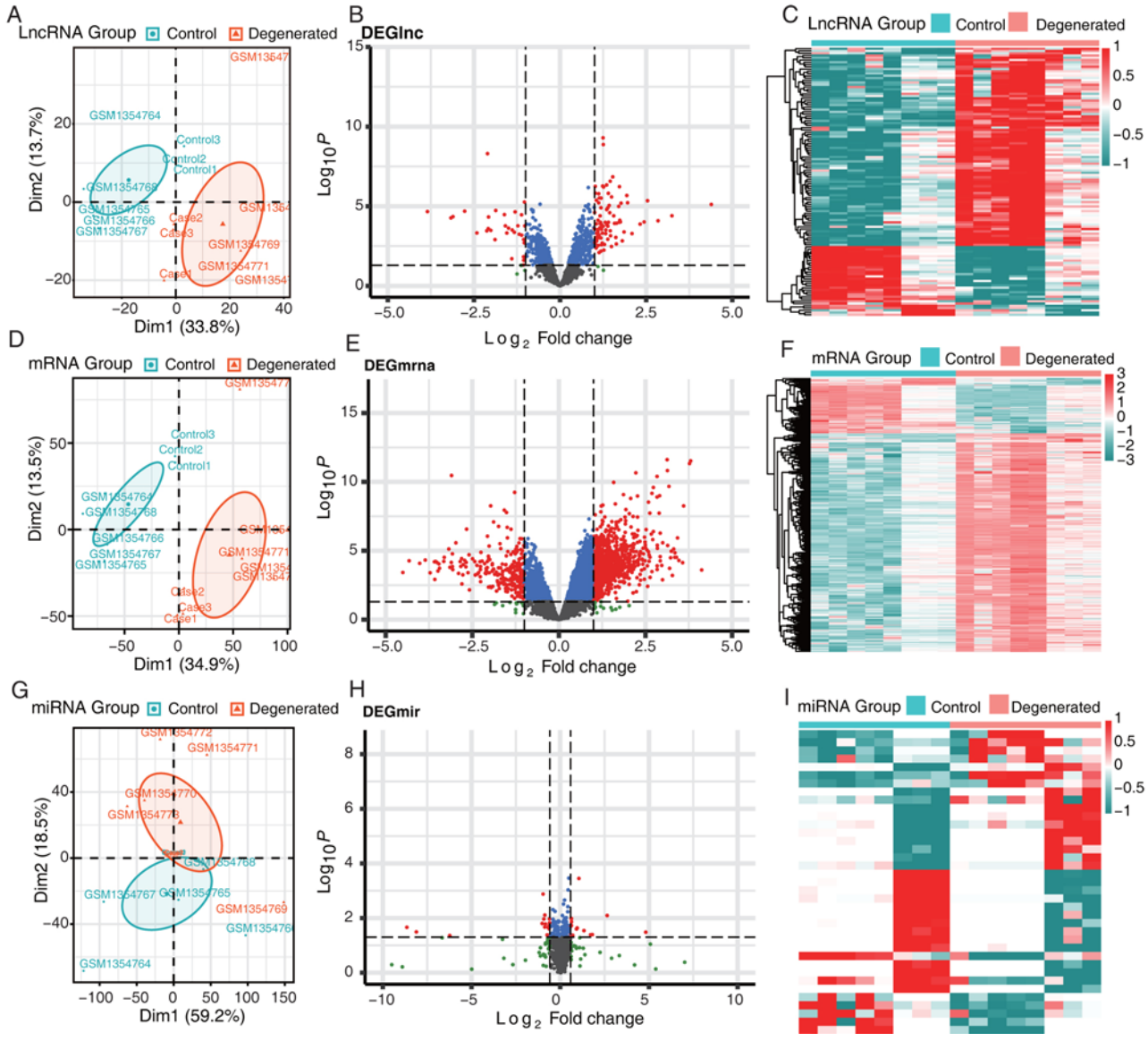

Figure 1. Principal Component Analysis (PCA), Volcano plot and heatmap for DELs (A, B and C), DEMs (D, E and F) and DEMs (G, H and I).

was collected. Datasets GSE56081[11] and GSE63492 were derived from an integrated microarray study that included lncRNA, miRNA, and mRNA profiles. GSE167199[12] comprised three degenerative NP tissue samples and three spinal cord injury samples as controls. Additionally, GSE134955 was used as an independent validation dataset. Detailed dataset information is presented in Table 1.

Differential Expression Analysis

The preprocessing pipeline was as follows: Whole transcript sequences were first downloaded from the GENCODE database (GENCODE v39, https://www.gencodegenes.org/). Microarray probes from the datasets were re-annotated by mapping them to lncRNA and mRNA transcripts using SeqMap v1.0.12[13] (https://jhui2014.github.io/seqmap/). After integration of RNA expression data, principal component analysis (PCA) was performed using the "FactoExtra" R package (https://github.com/kassambara/factoextra).

Batch effects were corrected using the "removeBatchEffect" function from the "limma" package[14], and PCA plots were generated with the "fviz_pca_ind" function. Differential expression analysis was then

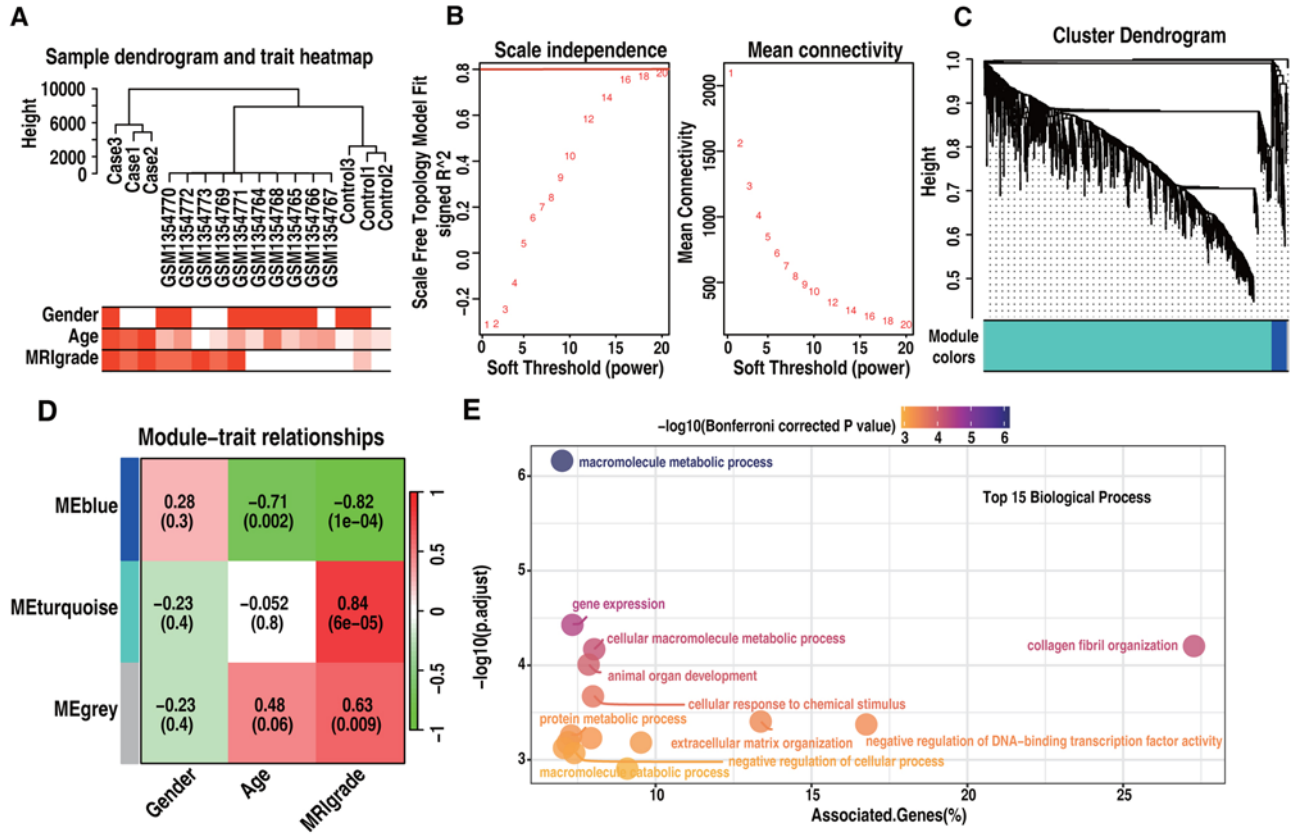

Figure 2. A. WGCNA sample dendrogram and trait heatmap. B. Soft threshold. C. Cluster Dendrogram for genes in modules. D. Module-trait relationships. E. Top15 Biological process enriched with genes in turquoise module.

conducted. For lncRNAs and mRNAs, differentially expressed DELs and DEMs were identified using a threshold of $p < 0.05$ and $|\log_2(\text{Fold Change})| > 1$. For DEMis, a threshold of $p < 0.05$ and $|\log_2(\text{Fold Change})| > 0.58$ was applied across each dataset.

WGCNA Algorithm

Weighted Gene Co-expression Network Analysis (WGCNA) version 1.61 [15] (https://cran.r-project.org/web/packages/WGCNA/) was used to identify gene modules associated with clinical phenotypes. The analysis parameters were set as follows: minModuleSize = 30 (each module containing at least 30 genes) and MEDissThres = 0.1 (modules with a similarity value greater than 0.9 were merged). Based on Pearson correlation analysis, modules significantly associated with MRI grade and age were identified.

Construction of the ceRNA Network

To identify RNA pairs related to MRI grade, the expression correlations between differentially expressed lncRNAs (DELs) and differentially expressed mRNAs (DEMs) were assessed using Spearman correlation analysis via the cor.test function in R (https://www.rdocumentation.org/packages/stats/versions/3.6.2/topics/cor.test). Statistical significance was adjusted using the Benjamini–Hochberg (BH) method, with thresholds set at FDR (false discovery rate) < 0.05 and |R| > 0.9.

Additionally, phenotype-associated RNA pairs were identified through Spearman correlation. DEM–DEMi pairs showing a significant negative correlation ($p < 0.05$ and $R < -0.5$) were selected and further validated using three miRNA target prediction databases: miRDB [16] (http://mirdb.org/index.html), miRTarBase[17] (https://mirtarbase.cuhk.edu.cn/~miRTarBase/miRTarBase_2022/php/index.php), and TargetScan[18] (https://www.targetscan.org/vert_80/).

The final ceRNA network was constructed by identifying intersecting mRNAs between lncRNA–mRNA and miRNA–mRNA interactions. These overlapping mRNAs were considered as potential key genes in IDD progression. The associated DELs and DEMis were included to construct the ceRNA regulatory network using Cytoscape v3.8.1[19]

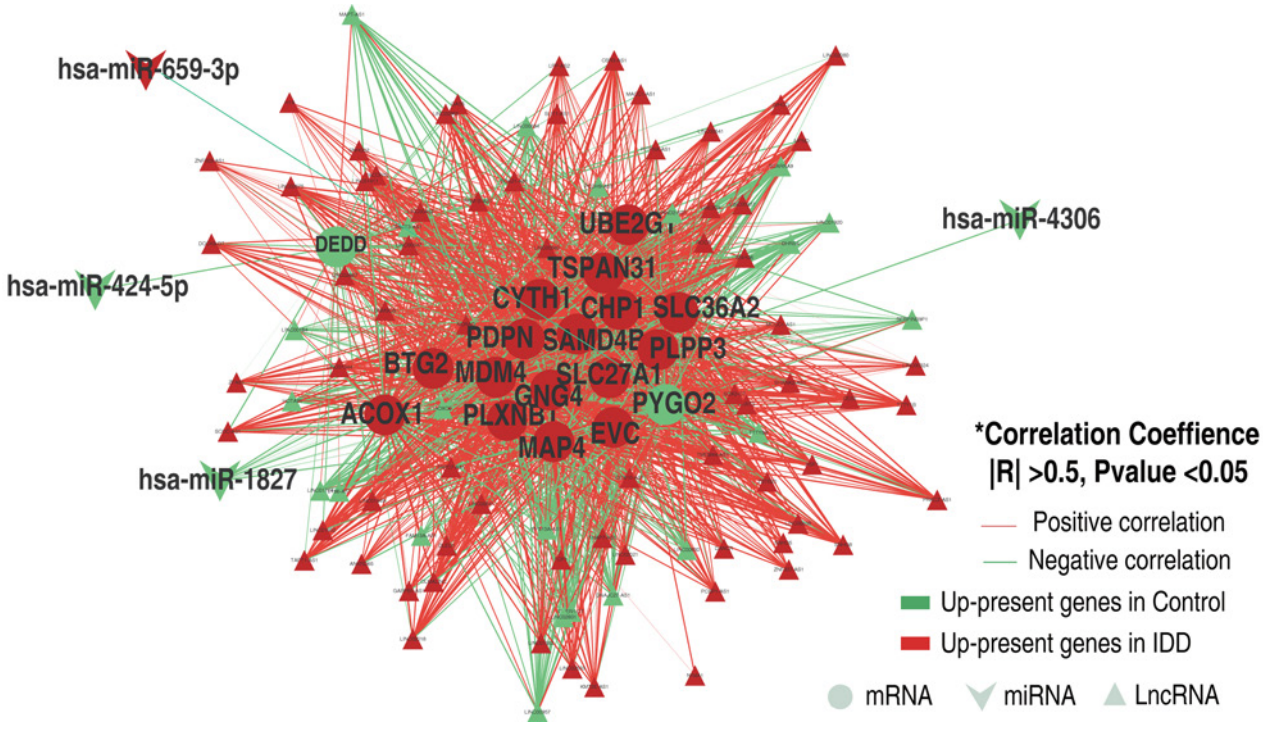

Figure 3. Core CeRNA network.

(https://cytoscape.org/).

To identify hub genes, CytoHubba[20] was used to analyze the topological features of the ceRNA network. The top 10% of nodes, ranked in descending order by Maximal Clique Centrality (MCC), were selected as core nodes. Corresponding subnetworks were then extracted from the ceRNA network for further analysis.

Least Absolute Shrinkage and Selection Operator (LASSO), Support Vector Machine (SVM), and Random Forest Algorithm

LASSO analysis was performed using the glmnet package in R. Support Vector Machine (SVM) and Random Forest algorithms were implemented using the e1071 package.

Results

Differentially Expressed lncRNAs, mRNAs, and miRNAs

Principal Component Analysis (PCA) demonstrated clear separation between degenerative and control sample groups, both before (Figure S1A–S1C) and after batch effect correction (Figure 1A, 1D, 1G). Compared with normal human nucleus pulposus (NP) tissue, a total of 119 differentially expressed DELs—88 upregulated and 31 downregulated—were identified (Figure 1B). Similarly, 1,267 differentially expressed DEMs, including 1,011 upregulated and 256 downregulated genes, were detected (Figure 1E). Additionally, 37 differentially expressed DEMis were identified, with 17 upregulated and 20 downregulated (Figure 1H). Hierarchical clustering analysis further confirmed significant differences in RNA expression profiles between degenerative and control samples (Figure 1C, 1F, 1I).

WGCNA Identifies IDD-Related Functional Modules

In the WGCNA network, hierarchical clustering of samples based on DEMs showed clear grouping of case and control samples following batch effect removal (Figure 2A). The soft-thresholding power parameter, which affects module independence and gene connectivity, was set to 20 based on scale-free topology criteria (Figure 2B). Using dynamic tree cutting, the differentially expressed genes were grouped into two co-expression modules: turquoise and blue (Figure 2C).

Correlation analysis revealed that both modules had significant associations with the MRI grade. Specifically, the blue module showed a positive correlation, while the turquoise module was negatively correlated (Figure 2D). Clinically, MRI is one of the most sensitive tools for evaluating IDD severity. Additionally, the blue module was significantly associated with age, whereas the turquoise module was exclusively correlated with MRI grade. Therefore, genes

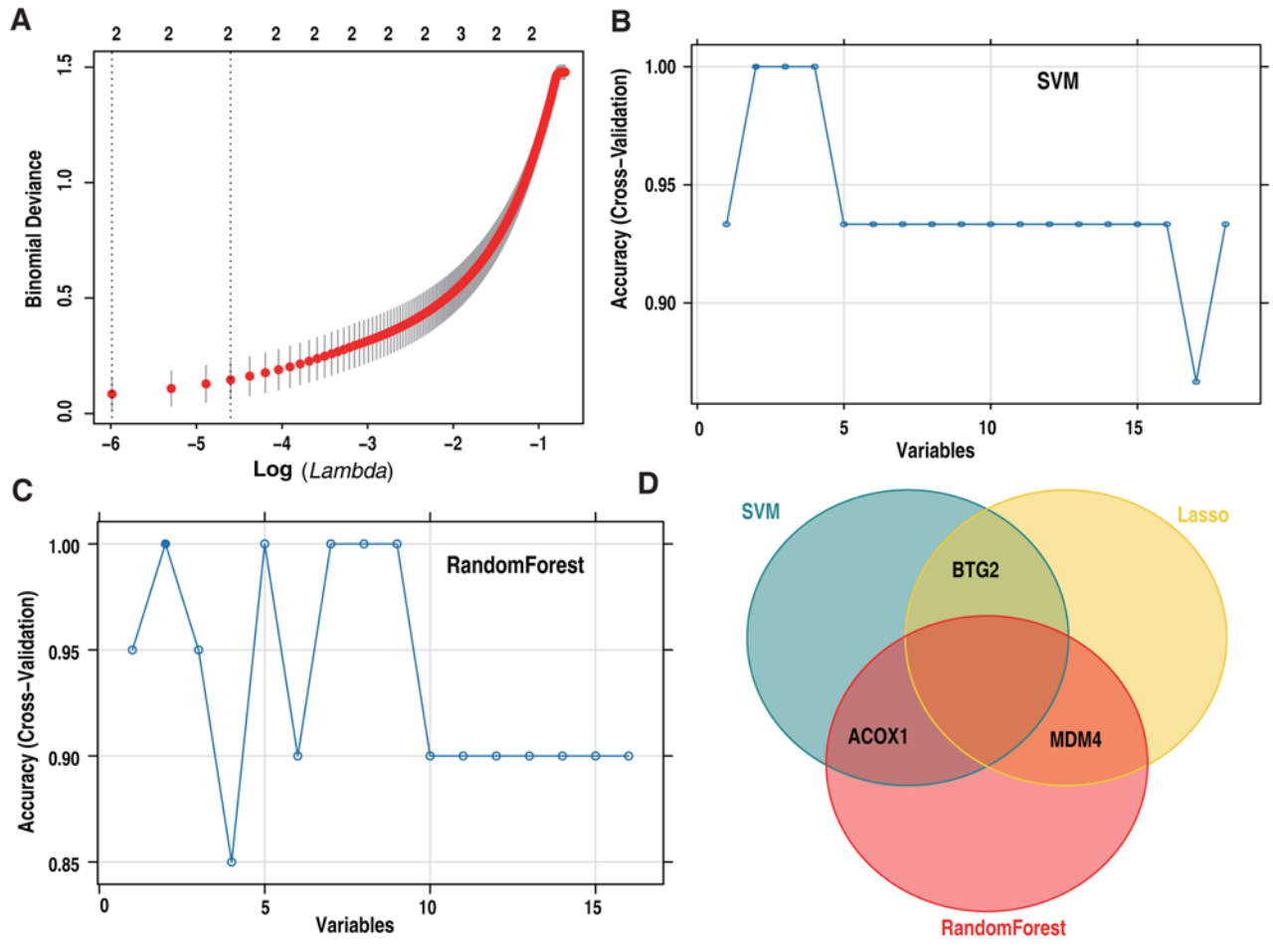

Figure 4. A Binomial Deviance plot for Lasso analysis. B. Accuracy-Variables plot for SVM. C. Accuracy-Variables plot for RandomForest. D. Venn plot for identified marker genes through 3 algorithms.

from both the blue and turquoise modules were selected for downstream analysis.

Functional Enrichment Analysis of Differentially Expressed RNAs

Functional enrichment analysis of genes in the turquoise module revealed significant involvement in several biological processes, including extracellular matrix organization, collagen fibril organization, response to cytokine, and cytokine-mediated signaling pathways (Figure 2E, Table S1). KEGG (Kyoto Encyclopedia of Genes and Genomes) pathway analysis further identified enrichment in pathways such as the Relaxin signaling pathway, Human T-cell leukemia virus 1 infection, and the AGE-RAGE signaling pathway in diabetic complications, among others (Table S1).

Construction of the ceRNA Network in IDD

Based on the defined criteria (FDR < 0.05 and |r| > 0.9), a total of 10,610 lncRNA–mRNA interaction pairs were identified. Using a threshold of $p < 0.05$ and $r < -0.5$, we detected 2,240 negatively correlated miRNA–mRNA pairs. By cross-referencing the miRDB[16], miRTarBase[17], and TargetScan[18] databases and retaining only those interactions supported by at least two databases, we identified 18 high-confidence negatively correlated miRNA–mRNA pairs, involving 4 differentially expressed DEMIs.

Notably, four miRNAs—hsa-miR-4306, hsa-miR-1827, hsa-miR-424-5p, and hsa-miR-659-3p—were significantly downregulated in IDD samples, suggesting their potential involvement in IDD progression.

By integrating validated miRNA–mRNA and lncRNA–mRNA interactions, a comprehensive ceRNA network comprising 18 mRNAs was constructed (Figure 3). From this network, LASSO analysis identified two key mRNAs—BTG2 and MDM4—as high-confidence markers (Figure 4A, Figure S1D, Figure 4D). SVM analysis further highlighted ACOX1 and BTG2 as having the highest classification accuracy (Figure 4B, Figure 4D), while Random Forest identified ACOX1 and MDM4 as top-performing markers (Figure 4C,

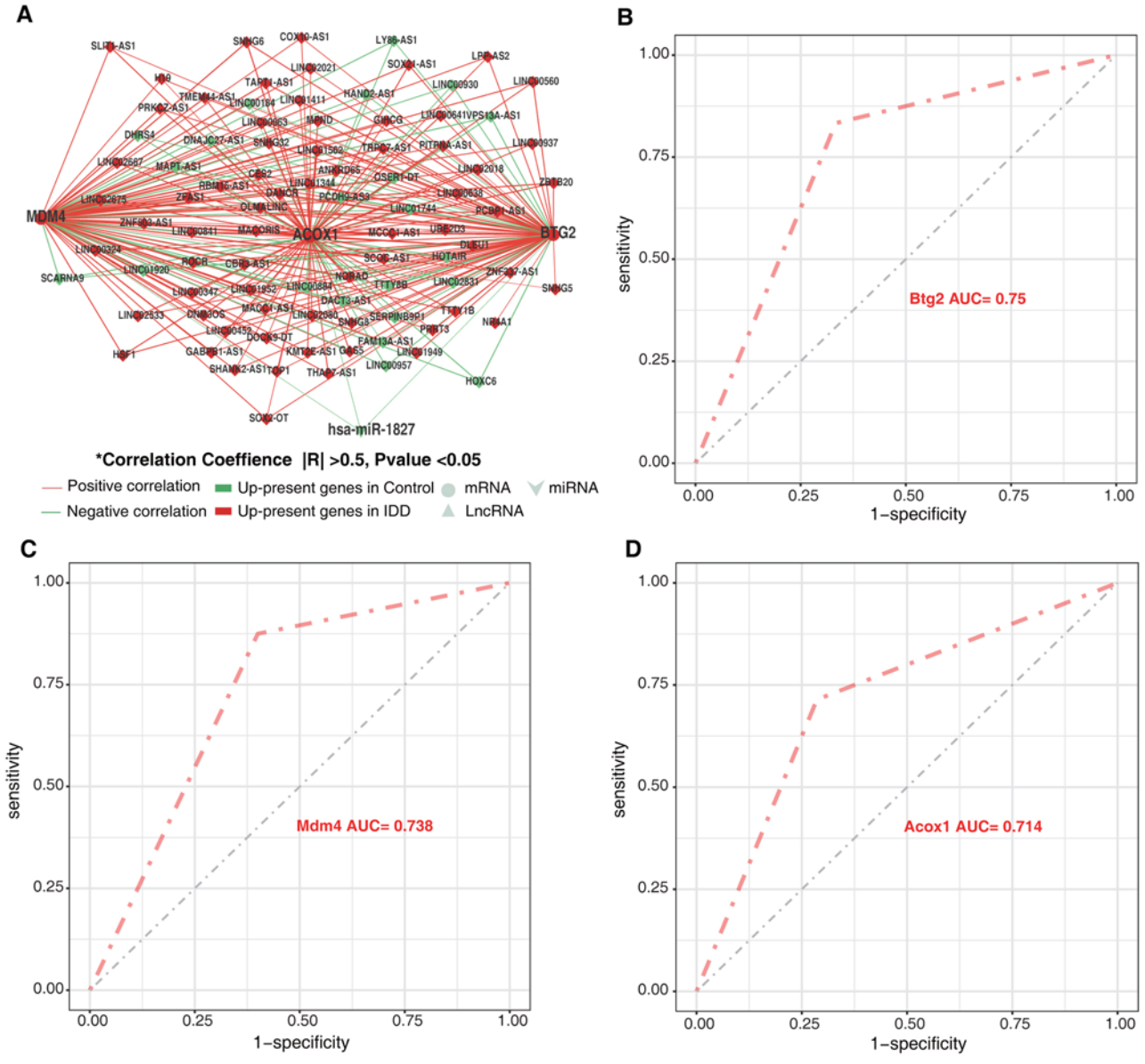

Figure 5. A. Core CeRNA network extracted just for ACOX1, BTG2 and MDM4, B. Validation ROC for Btg2 in another independent IDD data GSE134955. C. Validation ROC for Mdm4 in another independent IDD data GSE134955. D. Validation ROC for Acox1 in another independent IDD data GSE134955.

Figure 4D). These three genes were then used to extract a core ceRNA subnetwork to illustrate their regulatory roles in IDD (Figure 5A).

Discussion

Through integrative analysis of publicly available datasets, we identified numerous differentially expressed lncRNAs (DELs), mRNAs (DEMs), and miRNAs (DEMIs) in IDD samples compared with control cases. Functional enrichment analysis revealed that phenotype-related DEMs were primarily involved in macromolecule metabolic processes, collagen fibril organization, cellular response to chemical stimuli, and collagen-containing extracellular matrix components.

Furthermore, a ceRNA regulatory network was constructed to investigate the interactions among lncRNAs, miRNAs, and mRNAs. By applying three robust machine learning algorithms—LASSO, Support Vector Machine (SVM), and Random Forest—we identified three target

mRNAs, ACOX1, BTG2, and MDM4, which may serve as potential regulatory factors in IDD progression.

The ACOX1 gene encodes an enzyme involved in the fatty acid β-oxidation pathway, playing a key role in catalyzing the desaturation of acyl-CoAs to 2-trans-enoyl-CoAs. ACOX1 has been associated with aging and age-related disorders[21]. Although direct evidence linking ACOX1 to IDD is limited, it was identified as a target gene in the transcriptional regulatory network associated with the treatment of intervertebral disc degeneration using Duhuo Jisheng Decoction, suggesting its potential involvement in IDD pathogenesis[22].

BTG2 encodes a protein belonging to the BTG/Tob family, known for its anti-proliferative properties. Li et al.[23] demonstrated that BTG2, regulated by hsa-miR-185-5p, plays a significant role in IDD by influencing ECM metabolism and the immune response. Similarly, Wan et al.[24] reported that lincRNA-BTG2 was significantly associated with IDD and exhibited reduced expression in degenerative disc tissues.

Although the relationship between MDM4 and IDD is not well established, its role in regulating p53, a critical factor in maintaining IDD microenvironment homeostasis, has been documented[25]. MDM4 negatively regulates p53 expression[26]; therefore, elevated levels of MDM4 could suppress p53 activity and contribute to the dysregulation of the IDD microenvironment[25,26]. These findings suggest that MDM4 may serve as a potential target for IDD intervention.

Despite these promising findings, several limitations should be noted. First, due to the limited availability of exosome and IDD-specific transcriptomic datasets, the role of the identified mRNAs in disease progression requires validation in additional datasets. Second, as the results were derived solely from bioinformatics analyses, further experimental validation—including *in vitro* and *in vivo* studies—is essential to confirm these findings and elucidate the underlying molecular mechanisms.

In conclusion, several lncRNA/mRNAs/miRNA served as ceRNAs to regulate the pathogenesis of IDD in a miRNA-dependent manner. A ceRNA regulatory network was constructed and 3 newly identified crucial genes including ACOX1, BTG2 and MDM4 affecting IDD progression were identified. These findings provide novel insights in understanding the ceRNAs mechanism in IDD.

Authors' Contributions

Kai Huang, Huiqin Guan, Chao Liu, and Lingling Shen were responsible for the conception and design of the research. Lei Dai, Xiaogang Huang, Xinjun Zhang, and Xiaojun Xu contributed to data acquisition. Data analysis and interpretation were performed by Lei Dai, Xiaogang Huang, Xinjun Zhang, and Lingling Shen. Statistical analysis was conducted by Kai Huang, Huiqin Guan, and Xiaojun Xu. Funding was obtained by Kai Huang and Chao Liu. The manuscript was drafted by Kai Huang, Huiqin Guan, and Lingling Shen. Critical revision of the manuscript for important intellectual content was carried out by Kai Huang, Huiqin Guan, Chao Liu, and Xiaojun Xu. All authors read and approved the final manuscript.

Funding

This study was supported by the Program for Tackling Key Problems in Science and Technol-ogy in Songjiang District (No. 2024sjkjgg103) and College level project of Songjiang Hospital Affiliated to Shanghai Jiao Tong University School of Medicine (2023YJB-5).

References

1. Ravindra VM, Senglaub SS, Rattani A, Dewan MC, Härtl R, Bisson E, et al. Degenerative Lumbar Spine Disease: Estimating Global Incidence and Worldwide Volume. Global Spine J 2018;8(8):784-94.
2. Zehra U, Tryfonidou M, Iatridis JC, Illien-Jünger S, Mwale F, Samartzis D. Mechanisms and clinical implications of intervertebral disc calcification. Nat Rev Rheumatol 2022;9(10):022-00783.
3. Lu L, Xu A, Gao F, Tian C, Wang H, Zhang J, et al. Mesenchymal Stem Cell-Derived Exosomes as a Novel Strategy for the Treatment of Intervertebral Disc Degeneration. Front Cell Dev Biol 2022;9:770510.
4. Brosnan CA, Voinnet O. The long and the short of noncoding RNAs. Curr Opin Cell Biol 2009;21(3):416-25.
5. Catalanotto C, Cogoni C, Zardo G. MicroRNA in Control of Gene Expression: An Overview of Nuclear Functions. Int J Mol Sci 2016;17(10):1712.
6. Kung JT, Colognori D, Lee JT. Long noncoding RNAs: past, present, and future. Genetics 2013;193(3):651-69.
7. Yu Y, Zhang X, Li Z, Kong L, Huang Y. LncRNA HOTAIR suppresses TNF-α induced apoptosis of nucleus pulposus cells by regulating miR-34a/Bcl-2 axis. Biomed Pharmacother 2018;107:729-37.
8. Xi Y, Jiang T, Wang W, Yu J, Wang Y, Wu X, et al. Long non-coding HCG18 promotes intervertebral disc degeneration by sponging miR-146a-5p and regulating TRAF6 expression. Sci Rep 2017;7(1):017-13364.
9. Zhang Y, Xu Y, Feng L, Li F, Sun Z, Wu T, et al. Comprehensive characterization of lncRNA-mRNA related ceRNA network across 12 major cancers. Oncotarget 2016;7(39):64148-67.
10. Yao Y, Zhang T, Qi L, Zhou C, Wei J, Feng F, et al. Integrated analysis of co-expression and ceRNA network identifies five lncRNAs as prognostic markers for breast cancer. J Cell Mol Med 2019;23(12):8410-9.
11. Liu X, Che L, Xie YK, Hu QJ, Ma CJ, Pei YJ, et al. Noncoding RNAs in human intervertebral disc degeneration: An integrated microarray study. Genom Data 2015;5:80-1.
12. Li Z, Sun Y, He M, Liu J. Differentially-expressed mRNAs, microRNAs and long noncoding RNAs in intervertebral disc degeneration identified by RNA-sequencing. Bioengineered 2021;12(1):1026-39.
13. Jiang H, Wong WH. SeqMap: mapping massive amount of oligonucleotides to the genome. Bioinformatics 2008;24(20):2395-6.
14. Ritchie ME, Phipson B, Wu D, Hu Y, Law CW, Shi W, et

al. limma powers differential expression analyses for RNA-sequencing and microarray studies. Nucleic Acids Res 2015;43(7):20.
15. Langfelder P, Horvath S. WGCNA: an R package for weighted correlation network analysis. BMC Bioinformatics 2008;9(559):1471-2105.
16. Chen Y, Wang X. miRDB: an online database for prediction of functional microRNA targets. Nucleic Acids Res 2020;48(D1):D127-D31.
17. Huang HY, Lin YC, Li J, et al. miRTarBase 2020: updates to the experimentally validated microRNA-target interaction database. Nucleic Acids Res. 2020;48(D1):D148-D154.
18. McGeary SE, Lin KS, Shi CY, Pham TM, Bisaria N, Kelley GM, et al. The biochemical basis of microRNA targeting efficacy. Science 2019;366(6472):5.
19. Shannon P, Markiel A, Ozier O, Baliga NS, Wang JT, Ramage D, et al. Cytoscape: a software environment for integrated models of biomolecular interaction networks. Genome Res 2003;13(11):2498-504.
20. Chin CH, Chen SH, Wu HH, Ho CW, Ko MT, Lin CY. cytoHubba: identifying hub objects and sub-networks from complex interactome. BMC Syst Biol 2014;4(Suppl 4):1752-0509.
21. Vamecq J, Andreoletti P, El Kebbaj R, Saih FE, Latruffe N, El Kebbaj MHS, Lizard G, Nasser B, Cherkaoui-Malki M. Peroxisomal Acyl-CoA Oxidase Type 1: Anti-Inflammatory and Anti-Aging Properties with a Special Emphasis on Studies with LPS and Argan Oil as a Model Transposable to Aging. Oxid Med Cell Longev 2018;2018:6986984
22. Liu H, Li Y, Li Z, Li J, Zhang Q, Cao S, Li H. A Study Based on Network Pharmacology Decoding the Multi-Target Mechanism of Duhuo Jisheng Decoction for the Treatment of Intervertebral Disc Degeneration. Comput Intell Neurosci 2023;2023:7091407.
23. Li X, An Y, Wang Q, Han X. The new ceRNA crosstalk between mRNAs and miRNAs in intervertebral disc degeneration. Front Cell Dev Biol 2022;10:1083983.
24. Wan ZY, Song F, Sun Z, Chen YF, Zhang WL, Samartzis D, Ma CJ, Che L, Liu X, Ali MA, Wang HQ, Luo ZJ. Aberrantly expressed long noncoding RNAs in human intervertebral disc degeneration: a microarray related study. Arthritis Res Ther 2014;16(5):465.
25. Wang Y, Hu S, Zhang W, Zhang B, Yang Z. Emerging role and therapeutic implications of p53 in intervertebral disc degeneration. Cell Death Discov 2023;9(1):433.
26. Marine JC, Francoz S, Maetens M, Wahl G, Toledo F, Lozano G. Keeping p53 in check: essential and synergistic functions of Mdm2 and Mdm4. Cell Death Differ 2006;13(6):927-34.

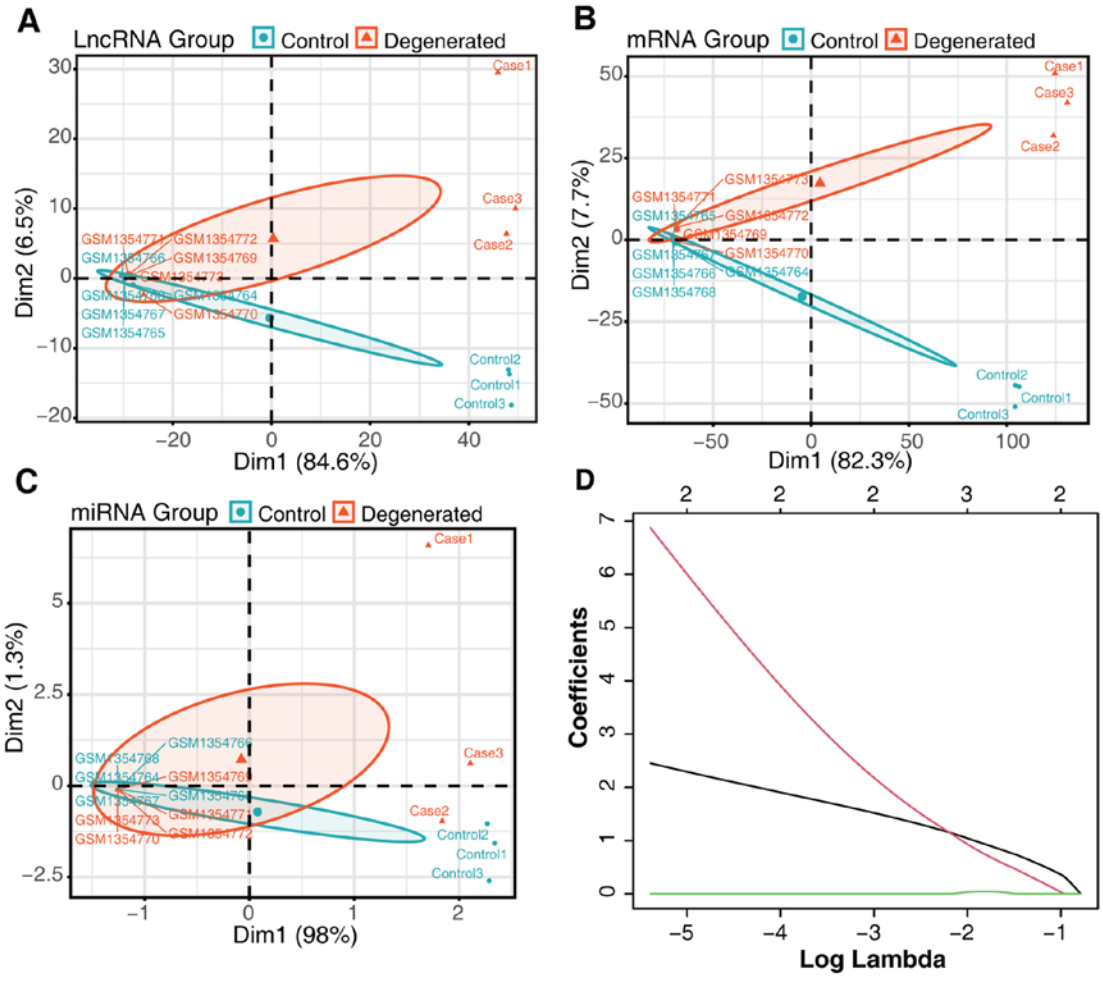

Figure S1. PCA of LncRNA(A), mRNA(B) and miRNA(C) before removing batch affection. D. Lasso coefficients.

Table Supplementary 1. Function analysis of genes in turquoise module.

ID	Term	P Value (Uncorrected)	P Value Corrected with Bonferroni	Number of Genes
GO:0043170	Macromolecule Metabolic Process	3.25×10^{-10}	6.88×10^{-7}	666
GO:0010467	Gene Expression	1.77×10^{-8}	3.74×10^{-5}	451
GO:0030199	Collagen Fibril Organization	2.96×10^{-8}	6.26×10^{-5}	18
GO:0044260	Cellular Macromolecule Metabolic Process	3.21×10^{-8}	6.77×10^{-5}	268
GO:0048513	Animal Organ Development	4.65×10^{-8}	9.83×10^{-5}	296
GO:0070887	Cellular Response to Chemical Stimulus	1.01×10^{-7}	0.000213	257
GO:0030198	Extracellular Matrix Organization	1.87×10^{-7}	0.000393	46
GO:0043433	Negative Regulation of DNA-Binding Transcription Factor Activity	2.01×10^{-7}	0.000423	30
GO:0019538	Protein Metabolic Process	2.62×10^{-7}	0.000552	410
GO:0010033	Response to Organic Substance	2.80×10^{-7}	0.000590	253
GO:0072359	Circulatory System Development	3.12×10^{-7}	0.000656	113
GO:0080090	Regulation of Primary Metabolic Process	3.15×10^{-7}	0.000661	442
GO:0019222	Regulation of Metabolic Process	3.57×10^{-7}	0.000749	499
GO:0048523	Negative Regulation of Cellular Process	4.03×10^{-7}	0.000848	370
GO:0009057	Macromolecule Catabolic Process	5.90×10^{-7}	0.001239	129
GO:0051090	Regulation of DNA-Binding Transcription Factor Activity	9.02×10^{-7}	0.001894	54
GO:1901575	Organic Substance Catabolic Process	1.78×10^{-6}	0.003732	184
GO:0048514	Blood Vessel Morphogenesis	2.01×10^{-6}	0.004212	70
GO:0060255	Regulation of Macromolecule Metabolic Process	3.32×10^{-6}	0.006945	457
GO:0048519	Negative Regulation of Biological Process	3.34×10^{-6}	0.006987	402
GO:1901564	Organonitrogen Compound Metabolic Process	3.36×10^{-6}	0.007018	468
GO:0048518	Positive Regulation of Biological Process	3.54×10^{-6}	0.007382	461
GO:0031323	Regulation of Cellular Metabolic Process	4.10×10^{-6}	0.008566	420
GO:1901360	Organic Cyclic Compound Metabolic Process	4.55×10^{-6}	0.009482	446
GO:0001944	Vasculature Development	5.86×10^{-6}	0.012218	78
GO:0051171	Regulation of Nitrogen Compound Metabolic Process	5.88×10^{-6}	0.012244	422
GO:0090304	Nucleic Acid Metabolic Process	5.88×10^{-6}	0.012255	380
GO:0016070	RNA Metabolic Process	5.90×10^{-6}	0.012294	344
GO:0006915	Apoptotic Process	7.38×10^{-6}	0.015340	167
GO:0012501	Programmed Cell Death	7.56×10^{-6}	0.015710	171
GO:0006139	Nucleobase-Containing Compound Metabolic Process	9.63×10^{-6}	0.020001	413
GO:0051172	Negative Regulation of Nitrogen Compound Metabolic Process	1.12×10^{-5}	0.023168	199
GO:0040012	Regulation of Locomotion	1.14×10^{-5}	0.023688	100
GO:0071310	Cellular Response to Organic Substance	1.16×10^{-5}	0.024003	200
GO:0035295	Tube Development	1.43×10^{-5}	0.029738	104
GO:0034641	Cellular Nitrogen Compound Metabolic Process	1.52×10^{-5}	0.031468	464
GO:0046483	Heterocycle Metabolic Process	1.55×10^{-5}	0.032137	422
GO:0010498	Proteasomal Protein Catabolic Process	1.59×10^{-5}	0.032875	57
GO:0010605	Negative Regulation of Macromolecule Metabolic Process	1.72×10^{-5}	0.035668	225
GO:0031099	Regeneration	1.83×10^{-5}	0.037912	29
GO:0009059	Macromolecule Biosynthetic Process	1.85×10^{-5}	0.038213	354
GO:0044265	Cellular Macromolecule Catabolic Process	2.06×10^{-5}	0.042473	96
GO:0043161	Proteasome-Mediated Ubiquitin-Dependent Protein Catabolic Process	2.14×10^{-5}	0.044242	51
GO:0042127	Regulation of Cell Population Proliferation	2.42×10^{-5}	0.049994	147
GO:0043227	Membrane-Bounded Organelle	4.74×10^{-20}	1.01×10^{-16}	937
GO:0043231	Intracellular Membrane-Bounded Organelle	8.50×10^{-19}	1.80×10^{-15}	876
GO:0043229	Intracellular Organelle	2.59×10^{-17}	5.49×10^{-14}	928
GO:0005737	Cytoplasm	1.13×10^{-16}	2.39×10^{-13}	860

Table Supplementary 1. *(Cont. from previous page).*

ID	Term	P Value (Uncorrected)	P Value Corrected with Bonferroni	Number of Genes
GO:0070013	Intracellular Organelle Lumen	2.43×10^{-12}	5.15×10^{-9}	455
GO:0062023	Collagen-Containing Extracellular Matrix	8.61×10^{-11}	1.82×10^{-7}	65
GO:0043202	Lysosomal Lumen	2.71×10^{-9}	5.74×10^{-6}	25
GO:0031012	Extracellular Matrix	1.95×10^{-7}	0.000410	69
GO:0005634	Nucleus	1.09×10^{-6}	0.002283	551
GO:0031981	Nuclear Lumen	1.42×10^{-6}	0.002979	347
GO:0005775	Vacuolar Lumen	1.64×10^{-6}	0.003428	30
GO:0005783	Endoplasmic Reticulum	6.04×10^{-6}	0.012570	175
GO:0022626	Cytosolic Ribosome	1.76×10^{-5}	0.036421	20
GO:0005654	Nucleoplasm	1.98×10^{-5}	0.040922	315
GO:0019899	Enzyme Binding	3.07×10^{-6}	0.006420	181
GO:0002020	Protease Binding	3.27×10^{-6}	0.006847	25
KEGG:04926	Relaxin Signaling Pathway	6.15×10^{-6}	0.012788	22